DMD Fast Forward. Published on June 27, 2012 as doi:10.1124/dmd.112.045187

Key Role of Nf-κB in the Cellular Pharmacokinetics of Adriamycin in MCF-7/Adr Cells: The Potential Mechanism for Synergy with 20(S)-Ginsenoside Rh2

Jingwei Zhang, Meng Lu, Fang Zhou, Haopeng Sun, Gang Hao, Xiaolan Wu, and Guangji Wang

Key Lab of Drug Metabolism and Pharmacokinetics, China Pharmaceutical University, Nanjing, Jiangsu, China (J.Z., M.L., F.Z., G.H., X.W., G.W.)

Department of Medicinal Chemistry, China Pharmaceutical University, Nanjing, Jiangsu, China (H.S.)

DMD Fast Forward. Published on June 27, 2012 as DOI: 10.1124/dmd.112.045187
This article has not been copyedited and formatted. The final version may differ from this version.

Running title: Nf-κB Regulates Cellular Pharmacokinetics of Adriamycin

Corresponding author: Prof. Guangji Wang, Key Lab of Drug Metabolism and Pharmacokinetics, China Pharmaceutical University, 24 Tong Jia Xiang, Nanjing, 210009, Jiangsu, China, E-mail addresses: guangjiwang@hotmail.com, Tel: 86-25-83271128. Fax: 86-25-83271060.

Number of text pages: 33

Number of tables: 0

Number of figures: 6

Number of references: 50

Number of words in the Abstract: 194

Number of words in the Introduction: 632

Number of words in the Discussion: 1253

Abbreviations

MDR, multi-drug resistance; LC-MS/MS, liquid chromatography tandem mass spectrometry; TBS/T, Tris-buffered saline/Tween 20; S.E., standard error; e.g., exempli gratia.

DMD Fast Forward. Published on June 27, 2012 as DOI: 10.1124/dmd.112.045187
This article has not been copyedited and formatted. The final version may differ from this version.

Abstract

We have previously demonstrated that ginsenoside 20(S)-Rh2 is a potent ABCB1 inhibitor and explored the cellular pharmacokinetic mechanisms for its synergistic effect on the cytotoxicity of adriamycin. The present studies were conducted to elucidate the key factors that influenced ABCB1 expression which could further alter adriamycin cellular pharmacokinetics. Meanwhile, the influence of 20(S)-Rh2 on the above factors was revealed for explaining its synergistic effect from the view of ABCB1 expression. The results indicated that 20(S)-Rh2 inhibited adriamycin-induced ABCB1 expression in MCF-7/Adr cells. Subsequent analyses indicated that 20(S)-Rh2 markedly inhibited adriamycin-induced activation of the MAPK/Nf-κB pathway, Nf-κB translocation to the nucleus and Nf-κB binding activity. Furthermore, 20(S)-Rh2 repressed the adriamycin-enhanced ability of Nf-κB to bind to the human MDR1 promoter, and MAPK/Nf-κB inhibitors and Nf-κB siRNA reversed the adriamycin-induced expression of ABCB1. Moreover, the cellular pharmacokinetics of adriamycin was also significantly altered by inhibiting Nf-κB. In conclusion, the MAPK/Nf-κB pathway mediates adriamycin-induced ABCB1 expression and subsequently alters the cellular pharmacokinetics of adriamycin. It was speculated that 20(S)-Rh2 acted on this pathway to lower adriamycin-induced ABCB1 expression in MCF-7/Adr cells, which provided mechanism-based support to the development of 20(S)-Rh2 as a multi-drug resistance (MDR) reversal agent.

Introduction

Inhibition or induction of ATP-binding cassette (ABC) transporters in tumor cells can lead to cellular pharmacokinetic alterations of many chemotherapeutic agents, which attracts much attention in cancer treatment (Hauswald et al., 2009; Kofla et al., 2011). ABCB1 is one of the extensively studied ABC transporters involved in adriamycin resistance of breast cancer (Kroger et al., 1999). Adriamycin is shown to have predominant nuclear accumulation in wild-type MDA-MB-435 cell lines, while it is sequestered away from the nucleus into cytoplasm in ABCB1-transduced MDA-MB-435 cell lines (Shen et al., 2008). The difference between the two types of cell lines in cellular pharmacokinetic behavior of adriamycin directly correlates with the sensitivity of these cells to the cytotoxic effects of adriamycin. Since ABCB1 is also found located in subcellular organelles, such as nuclei (Zhang et al., 2012), mitochondria (Solazzo et al., 2006), and the Golgi apparatus (Molinari et al., 1998), its role in subcellular pharmacokinetic behavior and anticancer activity of adriamycin has been well investigated and gained recognition (Zhang et al., 2012). Therefore, investigating the regulation of ABCB1 at the cell surface and in intracellular organelles in multi-drug resistance (MDR) tumor cells has great significances for breast cancer studies and treatment.

Many ABC transporter inhibitors have been found to promote the intracellular and subcellular distribution of anticancer agents by inhibiting transmembrane drug efflux, which enhances the binding ability of anticancer agent to its intracellular target and further strengthens its pharmacological effects (Shen et al., 2008; Shen et al.,

2009; Zhang et al., 2012). In addition to controlling the activities of ABC transporters, regulating the expressions of ABC transporters might broadly represent a more effective approach to overcoming MDR. ABC transporter expression could be generally classified as regulated at the transcriptional level (Scotto, 2003; Callaghan et al., 2008) and by post-translational modifications (Minami et al., 2009; Xie et al., 2010); transcriptional regulation has been a main focus of previous studies (Gu and Manautou, 2010). Many transcriptional factors including Nf-κB (Bentires-Alj et al., 2003), YB-1 (Shen et al., 2011), AP-1 (Bark and Choi, 2010) and HIF-1 (Han et al., 2007) have been found to bind to the promoter region of the MDR gene to initiate the transcription and expression of ABC transporters. Moreover, several signal transduction pathways have also been demonstrated to be involved in regulating the activities of those transcriptional factors, such as the MAPK (Katayama et al., 2007; Manov et al., 2007), PI3K (Barancik et al., 2006; Choi et al., 2008), PKC (Liu et al., 2009; Rigor et al., 2010) and Nf-κB (Hien et al., 2010; Kim et al., 2011) pathways. However, reports of signal molecules regulating the cellular pharmacokinetics of anticancer agents in cells are limited. Therefore, there is a pressing need to identify potential drugs that target specific key signal molecules to improve cellular pharmacokinetics of anticancer agents through regulating ABCB1 expression.

Ginsenoside Rh2, a protopanaxadiol type ginsenoside with a dammarane skeleton, is a trace active constituent of ginseng (Kitagawa et al., 1983). Many studies have demonstrated a remarkable synergistic effect of non-toxic Rh2 with anticancer agents in a variety of *in vitro* and *in vivo* tumor models (Kikuchi et al., 1991; Jia et al., 2004;

DMD Fast Forward. Published on June 27, 2012 as DOI: 10.1124/dmd.112.045187
This article has not been copyedited and formatted. The final version may differ from this version.

Xie et al., 2006). To fully understand this synergistic effect, we have previously demonstrated that Rh2 is a potent ABCB1 inhibitor *in vitro* and *in vivo* (Zhang et al., 2010). Then, cellular pharmacokinetic strategy was conducted to further illustrate the in-depth mechanisms. It was found that 20(S)-Rh2 improved the cellular pharmacokinetic behaviors and pharmacological effects of adriamycin in MCF-7/Adr cells via cellular/subcellular ABCB1 inhibition (Zhang et al., 2012).

The present studies intend to further elucidate the key factors which can affect ABCB1 expression and thus alter the cellular pharmacokinetic behaviors of adriamycin. Meanwhile, the synergistic mechanism of 20(S)-Rh2-mediated interference with these factors affecting ABCB1 expression was also examined

Materials and Methods

Reagents

20(S)-ginsenoside Rh2 (purity > 98%) was purchased from Jilin University (Changchun, China). SB203580 and U0126 were purchased from Cell Signaling Technology (Boston, MA, USA). SP600125, PD98059, PDTC, BAY 117082 and adriamycin were purchased from Sigma-Aldrich (St. Louis, MO). Monoclonal antibodies against p-p38, p-ERK, p-JNK, p38, ERK, JNK, p-Nf-κB p65, p-IκBα, p-IKKα/β, Nf-κB p65, IκBα, IKKα and IKKβ were purchased from Cell Signaling Technology (Boston, MA, USA). The monoclonal antibody against ABCB1 was purchased from Millipore (Millipore, USA). The antibodies for lamin B and β-actin were purchased from Boster Biological Technology (Wuhan, China). The horseradish

peroxidase-conjugated goat anti-mouse/rabbit IgG secondary antibodies were purchased from Cell Signaling Technology (Boston, MA, USA). Nf-κB p65 siRNAs were purchased from Santa Cruz Biotechnology (Santa Cruz, CA). Fugene® HD Transfection Reagent was purchased from Promega (Promega Corporation, USA). The electrophoretic mobility shift assay (EMSA) kit was purchased from Viagene Biotech (Viagene Biotech Inc., China). The SimpleChIP™ Enzymatic Chromatin IP Kit was purchased from Cell Signaling Technology (Boston, MA, USA). The SYBR® PrimeScript® RT-PCR Kit was purchased from Takara (Takara Bio, Japan). Deionized water was prepared by Milli-Q system (Millipore, Milford, MA, USA) and was used throughout.

Cell culture

The human breast cancer cells MCF-7 and adriamycin resistant human breast cancer cells MCF-7/Adr were obtained from the Institute of Hematology and Blood Diseases Hospital (Tianjin, China) and cultured in RPMI 1640 supplemented with 10% fetal bovine serum and 100 $U \cdot ml^{-1}$ penicillin and streptomycin (Invitrogen, Carlsbad, CA) at 37 ^{o}C with 5% CO_2. The cell medium was changed every other day. Cells were passaged upon reaching ~80% confluence. All of the cells used in this study were between passage 30 and 38, and were negative for mycoplasma infection.

Western Blotting Assay

For western blotting analysis, crude cell membranes were prepared as previously

described (Zhang et al., 2010). Nuclear and cytosolic extracts were isolated according to the KeyGen Nuclear Extract Kit (KeyGen Biotech, Nanjing, China). Protein concentrations were determined by the bicinchoninic acid method using the BCA protein assay kit (Pierce Chemical, Rockford, IL, USA). The protein samples were separated on an 8% SDS-polyacrlyamide gel and transferred onto a PVDF membrane (Bio-Rad, USA). The membrane was blocked with 5% non-fat milk in TBS/T for 1 h at 37 ^{o}C, and then incubated with the primary antibodies overnight at 4 ^{o}C. After washing, the membrane was incubated with horseradish peroxidase-conjugated secondary antibody for 1 h at 37 ^{o}C. The signals were detected using an enhanced chemiluminescence kit (Pierce Chemical, Rockford, IL, USA). The chemiluminescent signal was captured using a Bio-Rad ChemiDoc^{TM} XRS^{+} System (Bio-Rad, USA).

Electrophoretic mobility shift (EMSA) assay

The EMSA assay was performed as previously described (Wang et al., 2010). After drug treatment, nuclear extracts of MCF-7 and MCF-7/Adr cells were prepared and incubated with 1 μg of poly(dI-dC) in binding buffer for 30 min at 4 °C. DNA-binding activity was detected using a biotin-labeled oligonucleotide bio-Nf-κB probe (5'-GTAAGTTGAGGGGACTTTCCCAGGCCGT-3') and an EMSA kit according to the manufacturer's protocol. In competition assays, excess oligonucleotide probe (5'-AGTTGAGGGGACTTTCCCAGGC-3') or mutant probe (5'-AGTTGAGGCGAATGTCCCAGGC-3') was preincubated with nuclear extracts for 15 min at room temperature. In super shift assays, antibodies were added 30 min

before the biotin-labeled oligonucleotide. The resulting DNA–protein complex was separated from free oligonucleotide on a 6.5 % polyacrylamide gel containing 0.25 × TBE (Tris/borate/EDTA) buffer. The gels were dried, and the Nf-κB bands were analyzed by phosphoimaging using a CoolImger III (Viagene Biotech, Ningbo, China).

Pharmacophore Mapping and Molecular Docking

The pharmacophores of IKKβ inhibitors were generated by using the three dimensional quantitative structure-activity relationship (3D-QSAR) Pharmacophore Generation protocol implemented in the Discovery Studio package (Accelrys Inc., San Diego, CA) as we have previously described (Sun et al., 2011). Molecules that fit all of the features of the pharmacophore model were calculated for geometric fit values based on how well the molecules mapped onto the pharmacophoric feature location constraints and their deviation distances from the feature centers. A high fit value indicated a good match.

Molecular docking of IKKβ inhibitors to IKKβ was performed on the GOLD 3.01 program as we have previously described (Sun et al., 2011). This program employs a genetic algorithm in which the information regarding the ligand conformation and hydrogen bonding is encoded in a chromosome. In this study, the residues Leu21, Thr23, Gly24, Glu97, Cys99, Asp103, Lys147, Glu149, Asn150, and Glu172 and the surrounding residues within 6.5 Å were defined as the active site, which completely covered the ATP binding pocket of IKKβ.

DMD Fast Forward. Published on June 27, 2012 as DOI: 10.1124/dmd.112.045187
This article has not been copyedited and formatted. The final version may differ from this version.

Chromatin Immunoprecipitation (ChIP) - Quantitative Realtime Polymerase Chain Reaction (Q-PCR) Assays

A ChIP assay was performed using a SimpleChIP™ Enzymatic Chromatin IP Kit according to the manufacturer's protocol. Briefly, drug-treated cells were cross-linked with 1% formaldehyde in culture medium at room temperature for 10 min to preserve the protein-DNA interactions, followed by enzymatic digestion (micrococcal nuclease) and sonication to fragment the DNA into pieces of approximately 150–900 base pairs. Then, an antibody against Nf-κB p65 was added to precipitate the DNA transcriptome. The antibody-protein-DNA complexes were purified using ChIP-Grade Protein G magnetic beads. The DNA was further isolated from the complexes using a combination of heat to reverse the cross-linking and treatment with RNase and proteases; the DNA was then purified using DNA purification columns. The final ChIP DNAs were used as templates in a Q-PCR assay using the SYBR® PrimeScript® RT-PCR Kit. The primers for the human MDR1 gene were: (Forward) 5'-GCTGGGAAGATCGCTACTGA-3', (Reverse) 5'-GGTACCTGCAAACTCTGAGCA-3'. The resulting transcription values for each gene were normalized for primer pair amplification efficiency using the Q-PCR values obtained with input DNA (unprecipitated genomic DNA) as previously described (Chakrabarti et al., 2002; Rybtsova et al., 2007).

RNA Interference Assay

DMD Fast Forward. Published on June 27, 2012 as DOI: 10.1124/dmd.112.045187
This article has not been copyedited and formatted. The final version may differ from this version.

MCF-7/Adr cells were seeded on 6-well cell culture plates, incubated at 37 °C and transfected 24 h later at 70% confluence. Nf-κB p65 was transiently knocked down in MCF-7/Adr cells by Nf-κB p65 siRNA (h2) (Santa Cruz Biotechnology, sc-44212) targeting human Nf-κB p65 mRNA. Control siRNA-A (Santa Cruz Biotechnology, sc-37007), a non-targeting siRNA, was used as a negative control. The transfections were performed for 48 h according to the manufacturer's instructions for the Fugene® HD Transfection Reagent (Promega Corporation, USA). Then the cells were treated with adriamycin (10 μM) or 0.1% DMSO (control) for 24 h and collected for western blotting analysis.

Cellular Retention Assay

MCF-7/Adr cells were seeded on 24-well cell culture plates. The cells were treated with either Nf-κB p65 siRNAs to transiently knock down Nf-κB p65 (as described in RNA Interference Assay) or with Bay 117082 (25 μM) for 24 h to inhibit Nf-κB. Then, the drug-containing medium was discarded, the cells were washed, and 10 μM adriamycin was added. After incubation for the designated time (0.5, 1 and 2 h), the retention was stopped. The cells were lysed by three freeze-thaw cycles, and protein concentrations were measured using the Bradford method (Bradford, 1976). Adriamycin levels were determined by LC-MS/MS as we have previously described (Zhang et al., 2012). All experiments were conducted in triplicate.

Subcellular Distribution of Adriamycin in Live Cells

DMD Fast Forward. Published on June 27, 2012 as DOI: 10.1124/dmd.112.045187
This article has not been copyedited and formatted. The final version may differ from this version.

For direct observation of adriamycin subcellular distribution, MCF-7/Adr cells were seeded on 6-well cell culture plates and pre-treated with Nf-κB p65 siRNAs to transiently knock down Nf-κB p65 (as described in RNA Interference Assay). Before the experiment, the cells were stained with 5 μM Hoechst 33342 to label the nuclei. Then, the cells were treated as in the cellular retention assay. Images were collected at 0.5, 1 and 2 h after the addition of adriamycin using a fluorescence microscope (Leica, Germany) with identical settings for each study. The fluorescence of adriamycin (red) and Hoechst 33342 (blue) was observed through different filters respectively.

Cell Fractionation Approach for Quantification of the Adriamycin Subcellular Distribution

MCF-7/Adr cells were subcultured in 75 cm^2 cell culture flasks. Upon reaching ~90% confluence, the cultured cells were pre-treated with Bay 117082 (25 μM) for 24 h to inhibit Nf-κB. Then, the cells were treated as in the cellular retention assay. After incubation for the designated time (0.5, 1 and 2 h), the nuclei and mitochondria of the cells were isolated using the KeyGen Mitochondria/Nuclei Isolation Kit (Nanjing KeyGen Biotech. Co., LTD, China) as we have previously described (Zhang et al., 2012). The concentration of adriamycin in each subcellular component was determined by LC-MS/MS, and further adjusted to the concentrations based on the initial dosing volume. All of the experiments were conducted in triplicate.

Data Analysis

DMD Fast Forward. Published on June 27, 2012 as DOI: 10.1124/dmd.112.045187
This article has not been copyedited and formatted. The final version may differ from this version.

The data are expressed as the mean ± S.E. The statistical analyses included two-tailed Student's t-test and one-way ANOVA. The difference was considered to be statistically significant if the probability value was less than 0.05 ($p < 0.05$).

Results

20(S)-Rh2 Inhibited Adriamycin-induced ABCB1 Expression in MCF-7 and MCF-7/Adr cells

As shown in Fig. 1, the expression of ABCB1 in MCF-7/Adr cells was approximately 9-fold higher than that in MCF-7 cells. Incubation of MCF-7 and MCF-7/Adr cells with 10 μM adriamycin led to a further 1.8-fold increase in the expression of ABCB1 (Fig. 1). However, in the presence of 20(S)-Rh2 (1, 5, and 10 μM), the adriamycin-induced ABCB1 expression was significantly decreased in a concentration-dependent manner (Fig. 1).

20(S)-Rh2 Inhibited Adriamycin-mediated Activation of the MAPK Pathway in MCF-7/Adr Cells

As shown in Fig. 2A, when MCF-7/Adr cells were treated with 10 μM adriamycin, the phosphorylation of p38, JNK and ERK1/2 was markedly activated by 1.5-fold, 3.2-fold and 1.7-fold respectively. Furthermore, 20(S)-Rh2 (1, 5, and 10 μM) significantly suppressed the phosphorylation of these three MAP kinases induced by adriamycin in a concentration-dependent manner. The maximum inhibition of each MAP kinase upon treatment with 20(S)-Rh2 (10 μM) was approximately 60%.

DMD Fast Forward. Published on June 27, 2012 as DOI: 10.1124/dmd.112.045187
This article has not been copyedited and formatted. The final version may differ from this version.

20(S)-Rh2 Inhibited Adriamycin-mediated Activation of Nf-κB Pathway Signaling Molecules in MCF-7/Adr Cells

As shown in Fig. 2B, adriamycin (10 μM) significantly activated the phosphorylation of Iκb kinase β, which subsequently activated the phosphorylation of IκB. Phosphorylated IκB was ubiquitinated and degraded, which released Nf-κB dimers to translocate into the nucleus and be activated by phosphorylation. In the presence of 20(S)-Rh2 (1, 5, and 10 μM), the adriamycin-activated Nf-κB pathway was suppressed in a concentration-dependent manner. 20(S)-Rh2 inhibited the phosphorylation of Iκb kinase β and IκB, decreased Nf-κB and phosphorylation of Nf-κB, and prevented the translocation of Nf-κB into the nucleus.

20(S)-Rh2 Inhibited Adriamycin-enhanced Nf-κB Binding Activity in MCF-7 and MCF-7/Adr Cells

The EMSA results showed that adriamycin significantly enhanced the binding of Nf-κB to DNA in both MCF-7 and MCF-7/Adr cells. When the cells were treated with adriamycin plus 20(S)-Rh2 (1, 5, and 10 μM), the tight Nf-κB-DNA binding gradually weakened with increasing concentrations of 20(S)-Rh2 (Fig. 3A, lanes 1-14). The specificity of binding inhibition was demonstrated using cold consensus Nf-κB oligonucleotides, mutant Nf-κB oligonucleotides and different antibodies against Nf-κB. Excess cold consensus Nf-κB oligonucleotides competitively inhibited the binding of Nf-κB to the bio-NF-κB probe, while mutated Nf-κB oligonucleotides

DMD Fast Forward. Published on June 27, 2012 as DOI: 10.1124/dmd.112.045187
This article has not been copyedited and formatted. The final version may differ from this version.

had no effect. When antibodies against Nf-κB were added, the bands were shifted to higher molecule masses, suggesting that the adriamycin-activated complex consisted of p50 and p65 (Fig. 3B, lanes 15-26).

20(S)-Rh2 Mapped the Pharmacophore of IKKβ Inhibitors and Fitted the Homology Model of IKKβ

As shown in Fig. 4A, 20(S)-Rh2 mapped all of the critical pharmacophore features of IKKβ inhibitors. The fit value of 20(S)-Rh2 was 7.97, which was comparable to that of the positive compound 1 (fit value of 7.79). 20(S)-Rh2 mapped with the hydrophobic aromatic (light blue) of the pharmacophore through the isoamylene side chain and steroid parent ring. Furthermore, 20(S)-Rh2 was also docked into the binding site in the homology model of IKKβ (Fig. 4B). The analysis of the binding pattern of 20(S)-Rh2 with IKKβ indicated that 20(S)-Rh2 formed hydrogen-bonds with Glu149, Arg220, and Gln187 and adjoined the Leu21, Phe300, Phe26, Lys43, Val29 residues of IKKβ, which are all considered to be critical amino acids at the active sites of IKKβ.

20(S)-Rh2 Inhibited Adriamycin-enhanced Nf-κB Binding Ability to the Human MDR1 Promoter in MCF-7/Adr Cells

A ChIP-Q-PCR assay was performed to determine whether Nf-κB could bind to the MDR1 promoter. As shown in Fig. 5A, the level of Q-PCR product in the 10 μM adriamycin-treated group was 2-fold greater than that in control group, suggesting

DMD Fast Forward. Published on June 27, 2012 as DOI: 10.1124/dmd.112.045187
This article has not been copyedited and formatted. The final version may differ from this version.

adriamycin's functions in promoting Nf-κB binding to the MDR1 promoter. When the cells were treated with adriamycin plus 20(S)-Rh2, the Q-PCR product markedly decreased, indicating that 20(S)-Rh2 can weaken the Nf-κB binding to the MDR1 promoter.

Nf-κB Inhibitors Lowered Adriamycin-induced ABCB1 Expression in MCF-7/Adr Cells

As shown in Fig. 5B, treatment of MCF-7/Adr cells with 10 μM adriamycin for 24 h further elevated the expression of ABCB1 approximately 1.6-fold. When the cells were treated with adriamycin together with Nf-κB inhibitors, the adriamycin-induced ABCB1 expressions significantly decreased in a concentration-dependent manner.

Inhibition of Nf-κB Altered the Cellular Retention and Subcellular Distribution of Adriamycin in MCF-7/Adr Cells

As shown in Fig. 5C, inhibition of Nf-κB in MCF-7/Adr cells using the chemical inhibitor Bay 117082 (25 μM) caused the cellular accumulations of adriamycin to significantly increase approximately 3.8-fold over time. To further quantitatively analyze the adriamycin subcellular distribution in the presence or absence of Nf-κB, a cell fractionation approach was used to separate the nuclei and mitochondria in MCF-7/Adr cells treated with or without the Nf-κB chemical inhibitor Bay 117082 (25 μM) for 24 h. As shown in Fig. 5D, the accumulation of adriamycin in each subcellular organelle of MCF-7/Adr cells in the control group was as follows:

DMD Fast Forward. Published on June 27, 2012 as DOI: 10.1124/dmd.112.045187
This article has not been copyedited and formatted. The final version may differ from this version.

nuclei > mitochondria > cytosol. Inhibition of Nf-κB in MCF-7/Adr cells, caused accumulation of adriamycin in the nuclei, mitochondria and cytosol to significantly increase with time. The nucleus exhibited the highest accumulation of adriamycin, followed by the cytosol.

Silencing of Nf-κB p65 Decreased the ABCB1 Expression and Prevented Adriamycin-induced ABCB1 Expression in MCF-7/Adr Cells

As shown in Fig. 5E, Nf-κB p65 siRNA significantly reduced the expression of Nf-κB p65 in MCF-7/Adr cells to approximately 20% of the initial level. Silencing of Nf-κB p65 also directly led to a remarkable decrease in ABCB1 expression in MCF-7/Adr cells (Fig. 5F). Furthermore, silencing of Nf-κB p65 prevented adriamycin-induced ABCB1 expression in MCF-7/Adr cells (Fig. 5F).

Silencing of Nf-κB p65 Improved the Cellular Retention and Nuclear Distribution of Adriamycin in MCF-7/Adr Cells

Nf-κB p65 silencing in MCF-7/Adr cells led to a significant increase in the cellular accumulation of adriamycin over time (Fig. 5G). Specifically, uptake of adriamycin for 1 h and 2 h led to a marked 1.6-fold increase in the cellular accumulation of adriamycin. Moreover, as shown in Fig. 5H, little adriamycin (red fluorescence) entered the MCF-7/Adr cells or nuclei (blue fluorescence) at 0.5 h in the control and mock groups. Some weak red fluorescence was present around the nuclei of the cells in the control and mock group until 1 h and 2 h. The introduction of Nf-κB p65

DMD Fast Forward. Published on June 27, 2012 as DOI: 10.1124/dmd.112.045187
This article has not been copyedited and formatted. The final version may differ from this version.

siRNA into the MCF-7/Adr cells caused a significant enhancement in the rate and extent of adriamycin distribution in the nuclei. Silencing of Nf-κB p65 clearly accelerated the penetration of adriamycin into the nuclei (purple fluorescence) at 0.5 h after adriamycin addition, and caused a significant increase in adriamycin accumulation in the nuclei at 1 h and 2 h.

Discussion

Overexpression of ABCB1 is one of the main causes of MDR in cancer treatment because ABCB1 not only promotes the efflux of anticancer agents but also alters the subcellular distribution of anticancer agents within tumor cells; therefore, ABCB1 directly influences the effects of anticancer agents. Thus, regulation of ABCB1 expression potentially plays a key role in overcoming MDR (Bentires-Alj et al., 2003; Katayama et al., 2007).

In our previous studies, non-toxic concentrations of 20(S)-Rh2 exhibited a synergistic effect with adriamycin in MCF-7/Adr cells in MTT assays; this synergistic effect was attributed to the altered subcellular pharmacokinetics of adriamycin through inhibiting ABCB1 activity by 20(S)-Rh2 (Zhang et al., 2012). However, in the MTT assay, 20(S)-Rh2 was incubated with adriamycin for 72 h. During such a long period, ABCB1 expression, rather than ABCB1 activity, might also be regulated by 20(S)-Rh2. Therefore, the ABCB1 expression induced by adriamycin in the absence or presence of 20(S)-Rh2 was examined. As expected, 20(S)-Rh2 did inhibit adriamycin-induced ABCB1 expression (Fig. 1), which indicated that regulation of

DMD Fast Forward. Published on June 27, 2012 as DOI: 10.1124/dmd.112.045187
This article has not been copyedited and formatted. The final version may differ from this version.

ABCB1 expression might also contribute to the synergistic effect.

Considering that adriamycin acts as an anticancer agent by stimulating oxidative stress, the potential involvement of the MAPK and Nf-κB pathways in the regulation of ABCB1 expression became our focus (Bentires-Alj et al., 2003; Katayama et al., 2007; Kim et al., 2011; Shen et al., 2011) and the activities of MAPK and Nf-κB pathways were detected after the treatment of adriamycin with or without 20(S)-Rh2. In our experiment, treatment of MCF-7/Adr cells with adriamycin led to significant stimulation of the MAPK pathways, including p38, JNK and ERK (Fig. 2A). Similar adriamycin-induced MAPKs have also been observed in other cells *in vitro* and *in vivo* (Liu et al., 2008; Das et al., 2011; Xiao et al., 2012). The addition of 20(S)-Rh2 together with adriamycin led to marked inhibition of the adriamycin-induced MAPKs (Fig. 2A). Similar inhibitory effects of 20(S)-Rh2 on activated MAPKs have also been observed in human astroglioma cells stimulated by phorbol myristate acetate (Kim et al., 2007).

Through phosphorylation of MAPK signaling cascades, the subsequent downstream effectors (e.g. transcription factors) are finally activated (Crown, 2011). Nf-κB is an important transcriptional factor that regulates ABCB1 expression (Bentires-Alj et al., 2003), and a series of events directly relates to this regulatory course, including Nf-κB phosphorylation, translocation, and binding (Haddad and Abdel-Karim, 2011). The results indicated that adriamycin first stimulated the phosphorylation of IκB kinase β, which further led to the phosphorylation of IκB. Upon phosphorylation, IκB is released from the Nf-κB triple-complex, and the

DMD Fast Forward. Published on June 27, 2012 as DOI: 10.1124/dmd.112.045187
This article has not been copyedited and formatted. The final version may differ from this version.

p65-p50 dimer is freed to enter nucleus (Perkins, 2012). The addition of 20(S)-Rh2 together with adriamycin caused a marked inhibition of the adriamycin-stimulated phosphorylation of the above signaling molecules in the Nf-κB pathway (Fig. 2B). Similar results have also been observed upon treatment of human astroglial cells with the combination of tumor necrosis factor-α and 20(S)-Rh2 (Choi et al., 2007).

Upon entering the nucleus, the p65-p50 dimer binds to specific genes that have nearby DNA-binding sites for Nf-κB and then initiates gene expression. 20(S)-Rh2 has previously been reported to inhibit phorbol myristate acetate-activated Nf-κB binding ability in human astroglioma cells (Kim et al., 2007). However, no evidence regarding the effects of treating MCF-7/Adr cells with adriamycin and 20(S)-Rh2 has been found. Results from the EMSA assay demonstrated that the binding activities of Nf-κB were remarkably promoted by adriamycin and attenuated by 20(S)-Rh2 (Fig. 3A).

Although MAPK signaling cascades are generally considered to activate downstream effectors such as the transcription factors Nf-κB (Zhi et al., 2007; Li et al., 2010; Lin et al., 2011), it remains unclear about the relationship (parallel *vs*. causal) between the MAPK pathway and the Nf-κB pathway in MCF-7/Adr cells treated with adriamycin. Effects of p38, JNK and ERK inhibitors on adriamycin-activated Nf-κB pathway suggested that adriamycin stimulated Nf-κB pathway in a MAPK-dependent manner (supplementary Fig. 1). So it can be concluded that 20(S)-Rh2 interfered all the events in Nf-κB signal transduction pathway through MAPK pathway.

DMD Fast Forward. Published on June 27, 2012 as DOI: 10.1124/dmd.112.045187
This article has not been copyedited and formatted. The final version may differ from this version.

Pharmacophore mapping and molecular docking further indicated that 20(S)-Rh2 was a potential Nf-κB inhibitor. In our previous studies, a novel 3D-QSAR pharmacophore model was successfully developed and highlighted the important binding features of IKKβ ligands; a homology model of IKKβ was also established for further docking study (Sun et al., 2011). These two models provided deep insight into the characteristics of IKKβ inhibitors from ligand-based and structure-based methods. Hence, in our present research, 20(S)-Rh2 was evaluated using these two models, and good fitting values again proved that 20(S)-Rh2 was a potent Nf-κB inhibitor (Fig. 4).

ChIP-Q-PCR assay was next performed to clarify whether MAPK/Nf-κB pathway participated in regulating adriamycin-induced ABCB1 expression. Many Nf-κB binding sites have been reported at the human MDR1 promoter. One Nf-κB binding site (CCTTTCGGGG) is located in the first intron of the human MDR1 gene promoter (Bentires-Alj et al., 2003). Another Nf-κB binding site is located at position -6092 in the human MDR1 promoter (Kuo et al., 2002). Furthermore, Nf-κB and c-Fos have been reported to interact with the CAAT region (residues -116 to -113) of the MDR1 gene promoter (Ogretmen and Safa, 1999). Therefore, one Nf-κB binding site is proximal in the human MDR1 gene promoter. Thus, a PCR method can be used with human MDR1 gene primers to ascertain whether Nf-κB-binding DNA contains the human MDR1 gene and to perform further quantitative comparisons (Shen et al., 2010). In our ChIP-Q-PCR assay, an Nf-κB p65-specific antibody was used to preferentially precipitate DNA fragments containing the Nf-κB-binding region present

DMD Fast Forward. Published on June 27, 2012 as DOI: 10.1124/dmd.112.045187
This article has not been copyedited and formatted. The final version may differ from this version.

in the regulatory sequences of genes from MCF-7/Adr cells, and the MDR1 gene was chosen as our target gene. Adriamycin increased the binding of Nf-κB to MDR1 gene, and 20(S)-Rh2 significantly decreased this interaction (Fig. 5A). These assays indicated that adriamycin promoted Nf-κB binding to the MDR1 gene promoter to initiate its transcription, and 20(S)-Rh2 interfered with this interaction.

Many Nf-κB pathway inhibitors were then applied to adriamycin-treated MCF-7/Adr cells. It turned out that adriamycin-induced ABCB1 expression was significantly inhibited (to varying extents) in a concentration-dependent manner (Fig. 5B). MAPK pathway inhibitors also achieved similar effects (supplementary Fig. 2). These results were in accordance with previous reports of ABCB1 expression regulation (Katayama et al., 2007; Guo et al., 2008; Hien et al., 2010; Kim et al., 2011). As cellular pharmacokinetics of adriamycin was mainly determined by ABCB1 in MCF-7/Adr cells (supplementary Fig. 3), and Nf-κB inhibitors lowered ABCB1 expression, the cellular accumulation and nuclear distribution of adriamycin were significantly promoted by Nf-κB inhibitor (Fig. 5C and 5D). .

Due to the limited specificity of chemical inhibitors, siRNA (which has greater specificity) against NF-κB p65 was used. As expected, knockdown of Nf-κB p65 in MCF-7/Adr not only lowered the ABCB1 expression but also disabled the induction of ABCB1 expression by adriamycin (Fig. 5F). These assays supported a direct link between the MAPK/Nf-κB pathway and ABCB1 expression. Furthermore, knockdown of Nf-κB p65 caused the cellular accumulation and subcellular distribution of adriamycin to be significantly altered (Fig. 5G and 5H). These results

suggested that the alternation of ABCB1 expression at the cellular and subcellular level was mediated by the Nf-κB pathway.

In conclusion, the MAPK/Nf-κB pathway mediates adriamycin-induced ABCB1 expression and subsequently alters the cellular pharmacokinetics of adriamycin. 20(S)-Rh2 influenced this pathway to down-regulate adriamycin-induced ABCB1 expression in MCF-7/Adr cells (Fig. 6), which contributed to the improvement of adriamycin cellular pharmacokinetics and cytotoxicity. Our research highlights the key factors involved in the alternation of adriamycin cellular pharmacokinetics. It is helpful for the future development of MDR reversal agents with a cellular pharmacokinetic strategy.

DMD Fast Forward. Published on June 27, 2012 as DOI: 10.1124/dmd.112.045187
This article has not been copyedited and formatted. The final version may differ from this version.

Acknowledgements

The authors wish to sincerely thank post-graduates in Key Lab of Drug Metabolism and Pharmacokinetics (China Pharmaceutical University, Nanjing, China) for their kind assistance.

Authorship Contributions

Participated in research design: J.Z., F.Z., G.W..

Conducted experiments: J.Z., M.L., X.W..

Contributed new reagents or analytic tools: H.S., G.H., G.W..

Performed data analysis: J.Z., H.S., M.L..

Contributed to the writing of the manuscript: J.Z., F.Z., G.W..

References

Barancik M, Bohacova V, Sedlak J, Sulova Z, and Breier A (2006) LY294,002, a specific inhibitor of PI3K/Akt kinase pathway, antagonizes P-glycoprotein-mediated multidrug resistance. *Eur J Pharm Sci* **29:**426-434.

Bark H and Choi CH (2010) PSC833, cyclosporine analogue, downregulates MDR1 expression by activating JNK/c-Jun/AP-1 and suppressing NF-kappaB. *Cancer Chemother Pharmacol* **65:**1131-1136.

Bentires-Alj M, Barbu V, Fillet M, Chariot A, Relic B, Jacobs N, Gielen J, Merville MP, and Bours V (2003) NF-kappaB transcription factor induces drug resistance through MDR1 expression in cancer cells. *Oncogene* **22:**90-97.

Bradford MM (1976) A rapid and sensitive method for the quantitation of microgram quantities of protein utilizing the principle of protein-dye binding. *Anal Biochem* **72:**248-254.

Callaghan R, Crowley E, Potter S, and Kerr ID (2008) P-glycoprotein: so many ways to turn it on. *J Clin Pharmacol* **48:**365-378.

Chakrabarti SK, James JC, and Mirmira RG (2002) Quantitative assessment of gene targeting in vitro and in vivo by the pancreatic transcription factor, Pdx1. Importance of chromatin structure in directing promoter binding. *J Biol Chem* **277:**13286-13293.

Choi BH, Kim CG, Lim Y, Shin SY, and Lee YH (2008) Curcumin down-regulates the multidrug-resistance mdr1b gene by inhibiting the PI3K/Akt/NF kappa B pathway. *Cancer Lett* **259:**111-118.

Choi K, Kim M, Ryu J, and Choi C (2007) Ginsenosides compound K and Rh(2) inhibit tumor necrosis factor-alpha-induced activation of the NF-kappaB and JNK pathways in human astroglial cells. *Neurosci Lett* **421:**37-41.

Crown ED (2011) The role of mitogen activated protein kinase signaling in microglia and neurons in the initiation and maintenance of chronic pain. *Exp Neurol*.

Das J, Ghosh J, Manna P, and Sil PC (2011) Taurine suppresses doxorubicin-triggered oxidative stress and cardiac apoptosis in rat via up-regulation of PI3-K/Akt and inhibition of p53, p38-JNK. *Biochem Pharmacol* **81:**891-909.

Gu X and Manautou JE (2010) Regulation of hepatic ABCC transporters by xenobiotics and in disease states. *Drug Metab Rev* **42:**482-538.

Guo X, Ma N, Wang J, Song J, Bu X, Cheng Y, Sun K, Xiong H, Jiang G, Zhang B, Wu M, and Wei L (2008) Increased p38-MAPK is responsible for chemotherapy resistance in human gastric cancer cells. *BMC Cancer* **8:**375.

Haddad JJ and Abdel-Karim NE (2011) NF-kappaB cellular and molecular regulatory mechanisms and pathways: therapeutic pattern or pseudoregulation? *Cell Immunol* **271:**5-14.

Han HK, Han CY, Cheon EP, Lee J, and Kang KW (2007) Role of hypoxia-inducible factor-alpha in hepatitis-B-virus X protein-mediated MDR1 activation. *Biochem Biophys Res Commun* **357:**567-573.

Hauswald S, Duque-Afonso J, Wagner MM, Schertl FM, Lubbert M, Peschel C, Keller U, and Licht T (2009) Histone deacetylase inhibitors induce a very broad, pleiotropic anticancer drug resistance phenotype in acute myeloid leukemia cells by modulation of multiple ABC transporter genes. *Clin Cancer Res* **15:**3705-3715.

Hien TT, Kim HG, Han EH, Kang KW, and Jeong HG (2010) Molecular mechanism of suppression of MDR1 by puerarin from Pueraria lobata via NF-kappaB pathway and cAMP-responsive

element transcriptional activity-dependent up-regulation of AMP-activated protein kinase in breast cancer MCF-7/adr cells. *Mol Nutr Food Res* **54:**918-928.

Jia WW, Bu X, Philips D, Yan H, Liu G, Chen X, Bush JA, and Li G (2004) Rh2, a compound extracted from ginseng, hypersensitizes multidrug-resistant tumor cells to chemotherapy. *Can J Physiol Pharmacol* **82:**431-437.

Katayama K, Yoshioka S, Tsukahara S, Mitsuhashi J, and Sugimoto Y (2007) Inhibition of the mitogen-activated protein kinase pathway results in the down-regulation of P-glycoprotein. *Mol Cancer Ther* **6:**2092-2102.

Kikuchi Y, Sasa H, Kita T, Hirata J, Tode T, and Nagata I (1991) Inhibition of human ovarian cancer cell proliferation in vitro by ginsenoside Rh2 and adjuvant effects to cisplatin in vivo. *Anticancer Drugs* **2:**63-67.

Kim HG, Hien TT, Han EH, Hwang YP, Choi JH, Kang KW, Kwon KI, Kim BH, Kim SK, Song GY, Jeong TC, and Jeong HG (2011) Metformin inhibits P-glycoprotein expression via the NF-kappaB pathway and CRE transcriptional activity through AMPK activation. *Br J Pharmacol* **162:**1096-1108.

Kim SY, Kim DH, Han SJ, Hyun JW, and Kim HS (2007) Repression of matrix metalloproteinase gene expression by ginsenoside Rh2 in human astroglioma cells. *Biochem Pharmacol* **74:**1642-1651.

Kitagawa I, Yoshikawa M, Yoshihara M, Hayashi T, and Taniyama T (1983) [Chemical studies of crude drugs (1). Constituents of Ginseng radix rubra]. *Yakugaku Zasshi* **103:**612-622.

Kofla G, Turner V, Schulz B, Storch U, Froelich D, Rognon B, Coste AT, Sanglard D, and Ruhnke M (2011) Doxorubicin induces drug efflux pumps in Candida albicans. *Med Mycol* **49:**132-142.

Kroger N, Achterrath W, Hegewisch-Becker S, Mross K, and Zander AR (1999) Current options in treatment of anthracycline-resistant breast cancer. *Cancer Treat Rev* **25:**279-291.

Kuo MT, Liu Z, Wei Y, Lin-Lee YC, Tatebe S, Mills GB, and Unate H (2002) Induction of human MDR1 gene expression by 2-acetylaminofluorene is mediated by effectors of the phosphoinositide 3-kinase pathway that activate NF-kappaB signaling. *Oncogene* **21:**1945-1954.

Li MH, Kothandan G, Cho SJ, Huong PT, Nan YH, Lee KY, Shin SY, Yea SS, and Jeon YJ (2010) Magnolol Inhibits LPS-induced NF-kappaB/Rel Activation by Blocking p38 Kinase in Murine Macrophages. *Korean J Physiol Pharmacol* **14:**353-358.

Lin TH, Tang CH, Wu K, Fong YC, Yang RS, and Fu WM (2011) 15-deoxy-Delta(12,14) -prostaglandin-J2 and ciglitazone inhibit TNF-alpha-induced matrix metalloproteinase 13 production via the antagonism of NF-kappaB activation in human synovial fibroblasts. *J Cell Physiol* **226:**3242-3250.

Liu H, Yang H, Wang D, Liu Y, Liu X, Li Y, Xie L, and Wang G (2009) Insulin regulates P-glycoprotein in rat brain microvessel endothelial cells via an insulin receptor-mediated PKC/NF-kappaB pathway but not a PI3K/Akt pathway. *Eur J Pharmacol* **602:**277-282.

Liu J, Mao W, Ding B, and Liang CS (2008) ERKs/p53 signal transduction pathway is involved in doxorubicin-induced apoptosis in H9c2 cells and cardiomyocytes. *Am J Physiol Heart Circ Physiol* **295:**H1956-1965.

Manov I, Bashenko Y, Eliaz-Wolkowicz A, Mizrahi M, Liran O, and Iancu TC (2007) High-dose acetaminophen inhibits the lethal effect of doxorubicin in HepG2 cells: the role of P-glycoprotein and mitogen-activated protein kinase p44/42 pathway. *J Pharmacol Exp Ther* **322:**1013-1022.

Minami S, Ito K, Honma M, Ikebuchi Y, Anzai N, Kanai Y, Nishida T, Tsukita S, Sekine S, Horie T, and Suzuki H (2009) Posttranslational regulation of Abcc2 expression by SUMOylation system. *Am J Physiol Gastrointest Liver Physiol* **296:**G406-413.

Molinari A, Calcabrini A, Meschini S, Stringaro A, Del Bufalo D, Cianfriglia M, and Arancia G (1998) Detection of P-glycoprotein in the Golgi apparatus of drug-untreated human melanoma cells. *Int J Cancer* **75:**885-893.

Ogretmen B and Safa AR (1999) Negative regulation of MDR1 promoter activity in MCF-7, but not in multidrug resistant MCF-7/Adr, cells by cross-coupled NF-kappa B/p65 and c-Fos transcription factors and their interaction with the CAAT region. *Biochemistry* **38:**2189-2199.

Perkins ND (2012) The diverse and complex roles of NF-kappaB subunits in cancer. *Nat Rev Cancer* **12:**121-132.

Rigor RR, Hawkins BT, and Miller DS (2010) Activation of PKC isoform beta(I) at the blood-brain barrier rapidly decreases P-glycoprotein activity and enhances drug delivery to the brain. *J Cereb Blood Flow Metab* **30:**1373-1383.

Rybtsova N, Leimgruber E, Seguin-Estevez Q, Dunand-Sauthier I, Krawczyk M, and Reith W (2007) Transcription-coupled deposition of histone modifications during MHC class II gene activation. *Nucleic Acids Res* **35:**3431-3441.

Scotto KW (2003) Transcriptional regulation of ABC drug transporters. *Oncogene* **22:**7496-7511.

Shen F, Bailey BJ, Chu S, Bence AK, Xue X, Erickson P, Safa AR, Beck WT, and Erickson LC (2009) Dynamic assessment of mitoxantrone resistance and modulation of multidrug resistance by valspodar (PSC833) in multidrug resistance human cancer cells. *J Pharmacol Exp Ther* **330:**423-429.

Shen F, Chu S, Bence AK, Bailey B, Xue X, Erickson PA, Montrose MH, Beck WT, and Erickson LC (2008) Quantitation of doxorubicin uptake, efflux, and modulation of multidrug resistance (MDR) in MDR human cancer cells. *J Pharmacol Exp Ther* **324:**95-102.

Shen H, Xu W, Chen Q, Wu Z, Tang H, and Wang F (2010) Tetrandrine prevents acquired drug resistance of K562 cells through inhibition of mdr1 gene transcription. *J Cancer Res Clin Oncol* **136:**659-665.

Shen H, Xu W, Luo W, Zhou L, Yong W, Chen F, Wu C, Chen Q, and Han X (2011) Upregulation of mdr1 gene is related to activation of the MAPK/ERK signal transduction pathway and YB-1 nuclear translocation in B-cell lymphoma. *Exp Hematol* **39:**558-569.

Solazzo M, Fantappie O, Lasagna N, Sassoli C, Nosi D, and Mazzanti R (2006) P-gp localization in mitochondria and its functional characterization in multiple drug-resistant cell lines. *Exp Cell Res* **312:**4070-4078.

Sun HP, Zhu J, Chen FH, Zhang SL, Zhang Y, and You QD (2011) Combination of pharmacophore model development and binding mode analyses: identification of ligand features essential for IkappaB kinase-beta (IKKbeta) inhibitors and virtual screening based on it. *Eur J Med Chem* **46:**3942-3952.

Wang SJ, Gao Y, Chen H, Kong R, Jiang HC, Pan SH, Xue DB, Bai XW, and Sun B (2010) Dihydroartemisinin inactivates NF-kappaB and potentiates the anti-tumor effect of gemcitabine on pancreatic cancer both in vitro and in vivo. *Cancer Lett* **293:**99-108.

Xiao J, Sun GB, Sun B, Wu Y, He L, Wang X, Chen RC, Cao L, Ren XY, and Sun XB (2012) Kaempferol protects against doxorubicin-induced cardiotoxicity in vivo and in vitro. *Toxicology* **292:**53-62.

Xie X, Eberding A, Madera C, Fazli L, Jia W, Goldenberg L, Gleave M, and Guns ES (2006) Rh2

synergistically enhances paclitaxel or mitoxantrone in prostate cancer models. *J Urol* **175:**1926-1931.

Xie Y, Burcu M, Linn DE, Qiu Y, and Baer MR (2010) Pim-1 kinase protects P-glycoprotein from degradation and enables its glycosylation and cell surface expression. *Mol Pharmacol* **78:**310-318.

Zhang J, Zhou F, Wu X, Gu Y, Ai H, Zheng Y, Li Y, Zhang X, Hao G, Sun J, Peng Y, and Wang G (2010) 20(S)-ginsenoside rh2 noncompetitively inhibits p-glycoprotein in vitro and in vivo: a case for herb-drug interactions. *Drug Metab Dispos* **38:**2179-2187.

Zhang J, Zhou F, Wu X, Zhang X, Chen Y, Zha BS, Niu F, Lu M, Hao G, Sun Y, Sun J, Peng Y, and Wang G (2012) Cellular pharmacokinetic mechanisms of adriamycin resistance and its modulation by 20(S)-ginsenoside Rh2 in MCF-7/Adr cells. *Br J Pharmacol* **165:**120-134.

Zhi L, Ang AD, Zhang H, Moore PK, and Bhatia M (2007) Hydrogen sulfide induces the synthesis of proinflammatory cytokines in human monocyte cell line U937 via the ERK-NF-kappaB pathway. *J Leukoc Biol* **81:**1322-1332.

DMD Fast Forward. Published on June 27, 2012 as DOI: 10.1124/dmd.112.045187
This article has not been copyedited and formatted. The final version may differ from this version.

FOOTNOTES

J.Z., M.L. and F.Z. contributed equally to this work.

This work was supported by China National Nature Science Foundation [No. 30973583]; China 'Creation of New Drugs' Key Technology Projects [No. 2009ZX09304-001 and 2009ZX09502-004]; Jiangsu Province Nature Science Foundation [No. BE2010723 and BK2010437]; Fundamental Research Funds for the Central Universities [No. JKY2011072 and JKZ2011008].

DMD Fast Forward. Published on June 27, 2012 as DOI: 10.1124/dmd.112.045187
This article has not been copyedited and formatted. The final version may differ from this version.

Figures and legends

Fig. 1 Effects of 20(S)-Rh2 on adriamycin-induced ABCB1 expression in MCF-7 cells and MCF-7/Adr cells. The cells were treated with 20(S)-Rh2 (1, 5, and 10 μM) or vehicle in the presence of 10 μM adriamycin. Cellular membrane and cytoplasmic fractions were prepared using lysis buffer and subjected to western blotting with the indicated antibodies. Top: representative blots. Bottom: the bar graph that shows the quantification of the band intensity. The data are expressed as the mean ± S.E. (n=3, # $p < 0.05$ *vs.* control group; * $p < 0.05$ *vs.* adriamycin group)

Fig. 2 Effects of 20(S)-Rh2 on adriamycin-mediated activation of the MAPK pathway (A) and Nf-κB pathway (B) in MCF-7/Adr cells. MCF-7/Adr cells were treated with 20(S)-Rh2 (1, 5, and 10 μM) or vehicle in the presence of 10 μM adriamycin. Nuclear and cytoplasmic fractions were then prepared using lysis buffer and subjected to western blotting with the indicated antibodies. ## $p < 0.01$ *vs.* control group; * $p < 0.05$ *vs.* adriamycin group.

Fig. 3 Effects of 20(S)-Rh2 on adriamycin-mediated activation of Nf-κB binding ability in MCF-7 cells and MCF-7/Adr cells. (A) MCF-7 cells (left panel) and MCF-7/Adr (right panel) cells were treated with 20(S)-Rh2 (1, 5, and 10 μM) or vehicle in the presence of 10 μM adriamycin. Nuclear extracts from the cells were then labeled with an Nf-κB probe for an EMSA assay. (B) Nuclear extracts from adriamycin-activated MCF-7 cells (left panel) and MCF-7/Adr (right panel) cells were

DMD Fast Forward. Published on June 27, 2012 as DOI: 10.1124/dmd.112.045187
This article has not been copyedited and formatted. The final version may differ from this version.

labeled with an Nf-κB probe plus various Nf-κB probe competitors. The lanes represent the following: solvent control (1, 8), adriamycin 10 μM (2, 9, 16, 22), adriamycin 10 μM + 20(S)-Rh2 1 μM (3, 10), adriamycin 10 μM + 20(S)-Rh2 5 μM (4, 11), adriamycin 10 μM + 20(S)-Rh2 10 μM (5, 12), positive control (6, 13), negative control (7, 14, 15, 21), cold oligonucleotide probe (17, 23), mutant oligonucleotide probe (18, 24), p65 antibody (19, 25) and p50 antibody (20, 26).

Fig. 4 (A) Mapping of 20(S)-Rh2 with the pharmacophores of IKKβ inhibitors. Hypothesized features are color-coded as follows: light blue, hydrophobic aromatic; violet, hydrogen bond donor; and green, hydrogen bond acceptor. (B) Molecular docking of 20(S)-Rh2 to the homology model of IKKβ. Green dotted line, hydrogen bond. (C) Structure of 20(S)-Rh2. (D) Structure of compound 1, a positive inhibitor of IKKβ inhibitor.

Fig. 5 (A) Effects of 20(S)-Rh2 on adriamycin-mediated activation of Nf-κB binding to the human MDR1 gene in MCF-7/Adr cells. (B) Effects of Nf-κB inhibitors on adriamycin-induced ABCB1 expression in MCF-7/Adr cells. (C) Effects of the Nf-κB chemical inhibitor Bay 117082 on the accumulation of adriamycin in MCF-7/Adr cells. (D) Effects of the Nf-κB chemical inhibitor Bay 117082 on adriamycin subcellular distribution using a cell fractionation approach. (E) Knockdown of Nf-κB p65 in MCF-7/A using siRNA. (F) Effects of adriamycin on ABCB1 expression in control MCF-7/Adr cells and upon silencing of Nf-κB p65. (G) Effects of Nf-κB p65

DMD Fast Forward. Published on June 27, 2012 as DOI: 10.1124/dmd.112.045187
This article has not been copyedited and formatted. The final version may differ from this version.

siRNA on the accumulation of adriamycin in MCF-7/Adr cells. (H) Effects of Nf-κB p65 siRNA on adriamycin nuclear distribution in MCF-7/Adr cells. The data are expressed as the mean ± S.E. (n=3, # $p < 0.05$, ## $p < 0.01$ *vs.* control group; * $p < 0.05$, ** $p < 0.01$ *vs.* adriamycin group; ‡ $p < 0.05$, ‡‡ $p < 0.01$ between Nf-κB p65 siRNA group *vs.* corresponding mock group; † $p < 0.05$ between mock group *vs.* mock group plus adriamycin)

Fig. 6 Proposed cell signal transduction pathways for adriamycin-induced ABCB1 expression in MCF-7/Adr cells and the potential mechanisms for the inhibitory effect of 20(S)-Rh2 on adriamycin-induced ABCB1 expression.

Fig 1

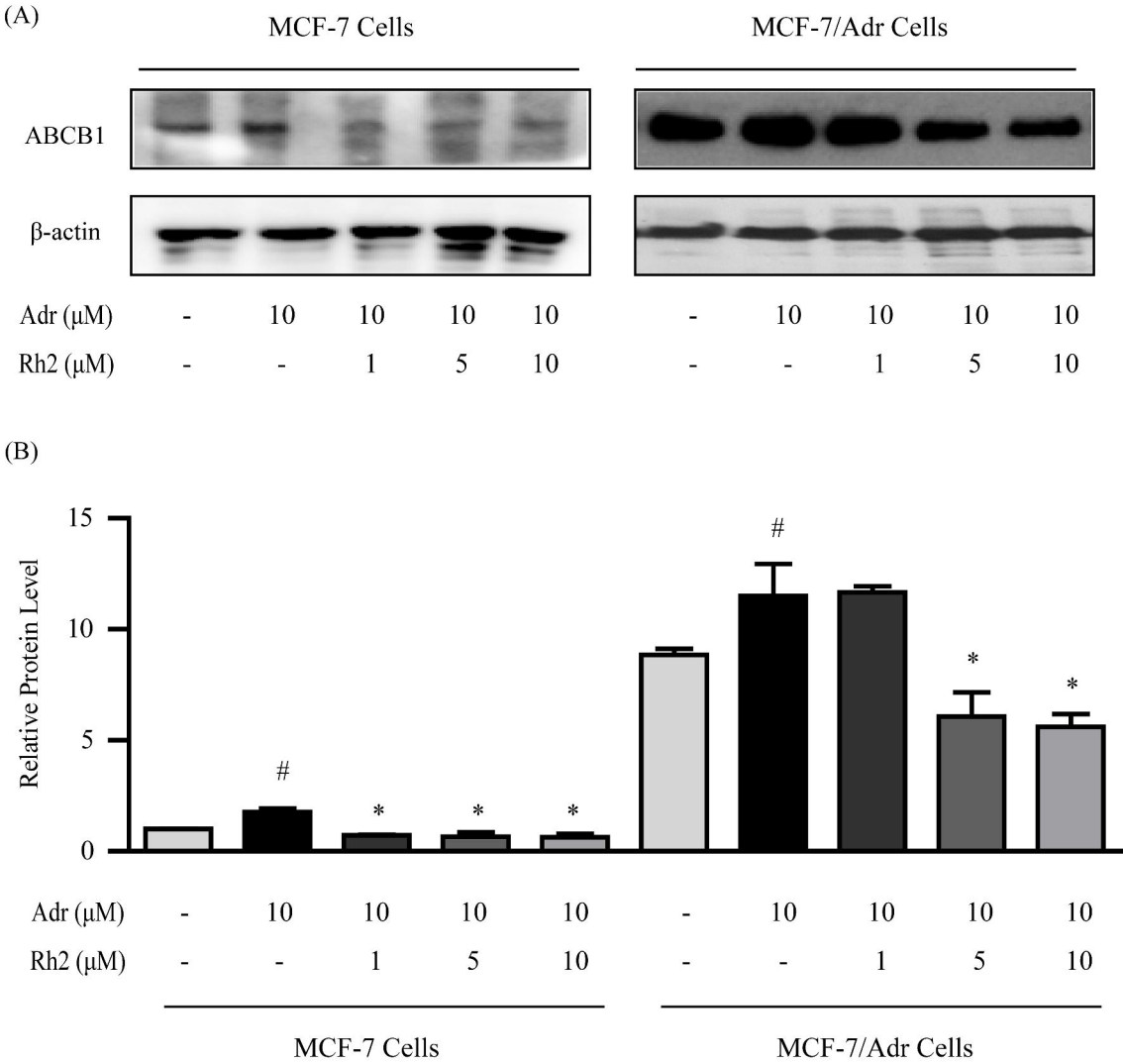
(A)
MCF-7 Cells
MCF-7/Adr Cells
ABCB1
β-actin
Adr (μM) - 10 10 10 10 - 10 10 10 10
Rh2 (μM) - - 1 5 10 - - 1 5 10
(B)
Relative Protein Level
15
10
5
0
#
*
Adr (μM) - 10 10 10 10 - 10 10 10 10
Rh2 (μM) - - 1 5 10 - - 1 5 10
MCF-7 Cells
MCF-7/Adr Cells

Fig 2

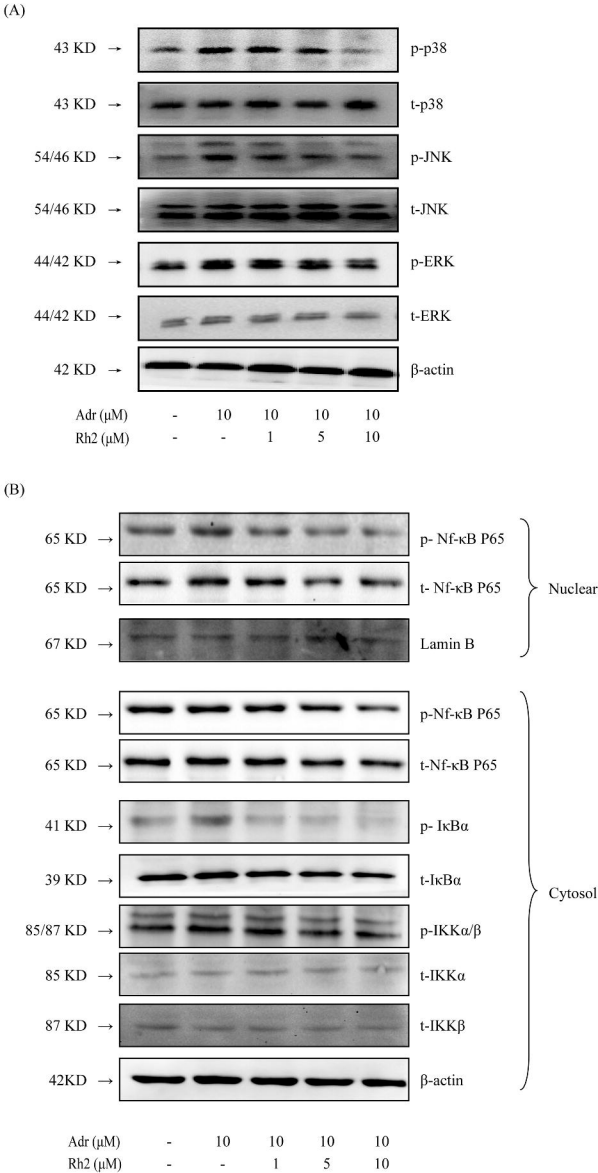
(A)
43 KD →
p-p38
43 KD →
t-p38
54/46 KD →
p-JNK
54/46 KD →
t-JNK
44/42 KD →
p-ERK
44/42 KD →
t-ERK
42 KD →
β-actin
Adr (μM) - 10 10 10 10
Rh2 (μM) - - 1 5 10
(B)
65 KD →
p- Nf-κB P65
65 KD →
t- Nf-κB P65
Nuclear
67 KD →
Lamin B
65 KD →
p-Nf-κB P65
65 KD →
t-Nf-κB P65
41 KD →
p- IκBα
39 KD →
t-IκBα
85/87 KD →
p-IKKα/β
85 KD →
t-IKKα
87 KD →
t-IKKβ
Cytosol
42KD →
β-actin
Adr (μM) - 10 10 10 10
Rh2 (μM) - - 1 5 10

Fig 3

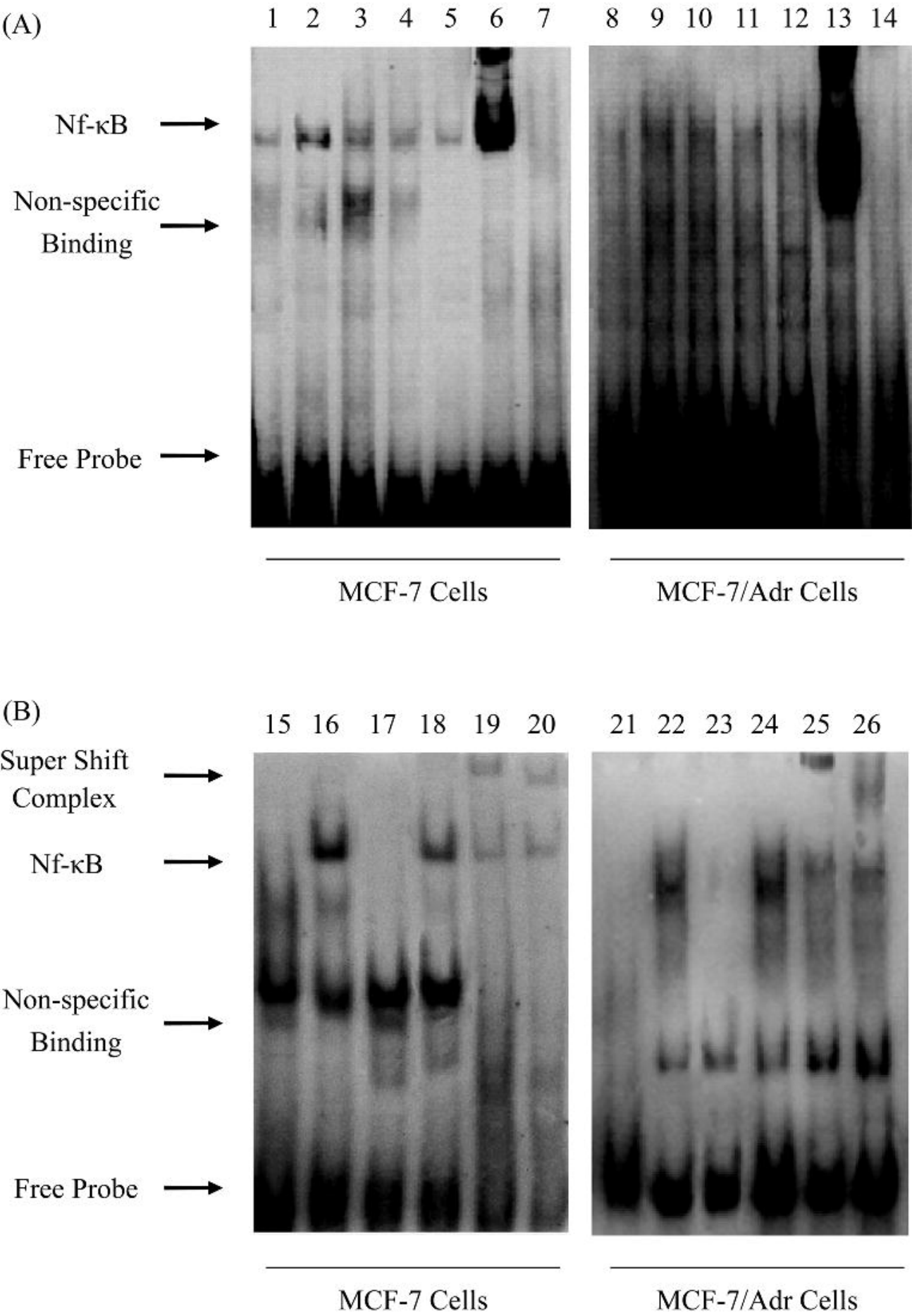
(A)
1 2 3 4 5 6 7
8 9 10 11 12 13 14
Nf-κB
Non-specific Binding
Free Probe
MCF-7 Cells
MCF-7/Adr Cells
(B)
15 16 17 18 19 20
21 22 23 24 25 26
Super Shift Complex
Nf-κB
Non-specific Binding
Free Probe
MCF-7 Cells
MCF-7/Adr Cells

Fig 4

(A)

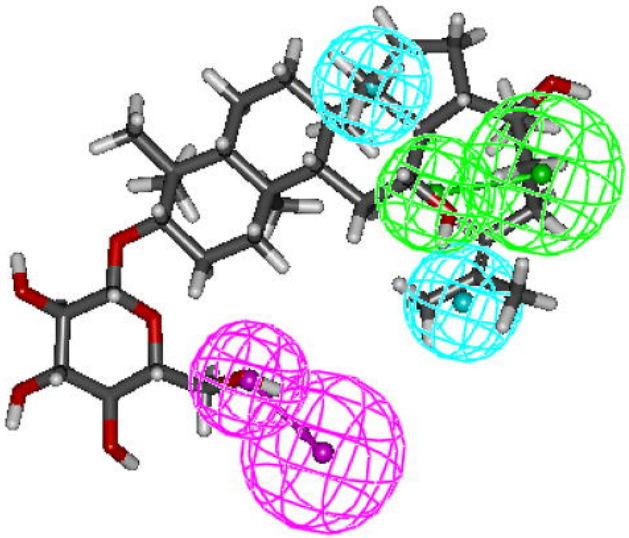

(C)

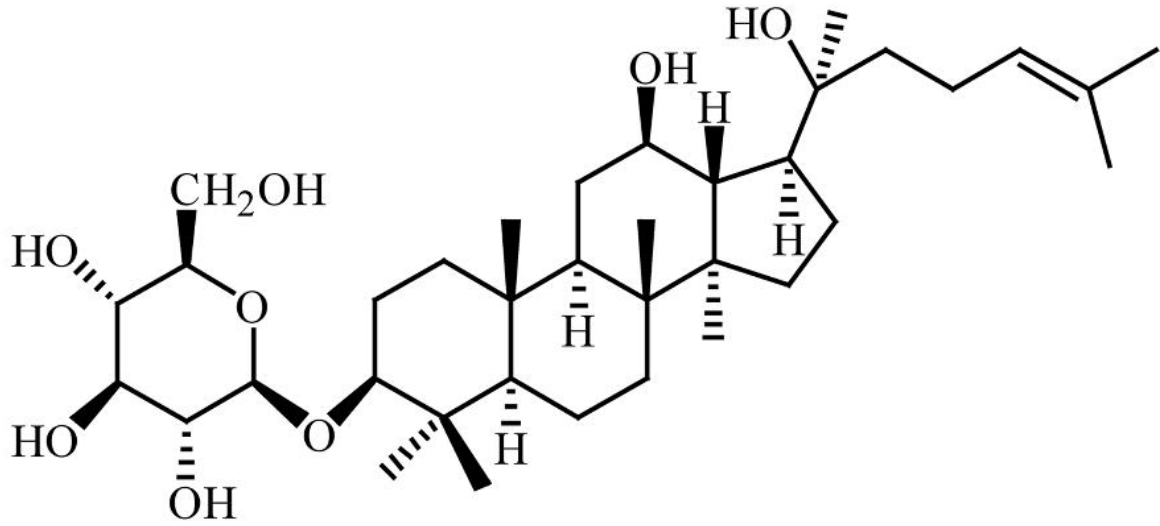
HO
OH
H
CH2OH
HO
O
H
H
HO
O
H
OH

(B)

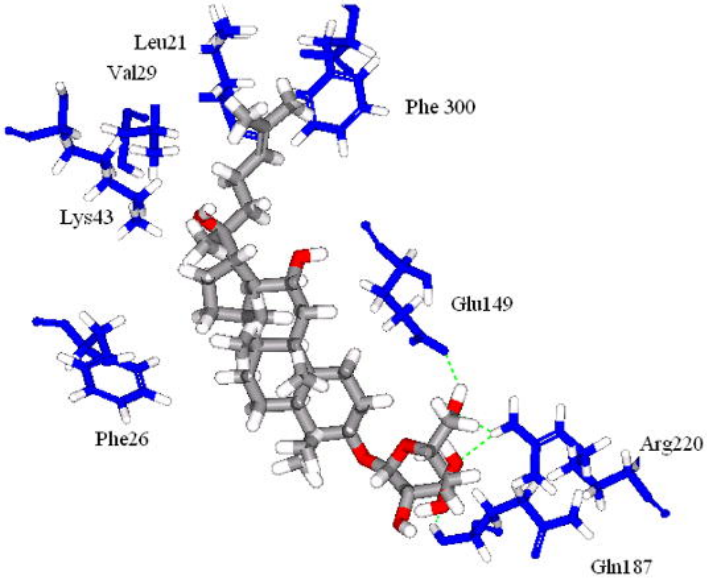
Leu21
Val29
Phe 300
Lys43
Glu149
Phe26
Arg220
Gln187

(D)

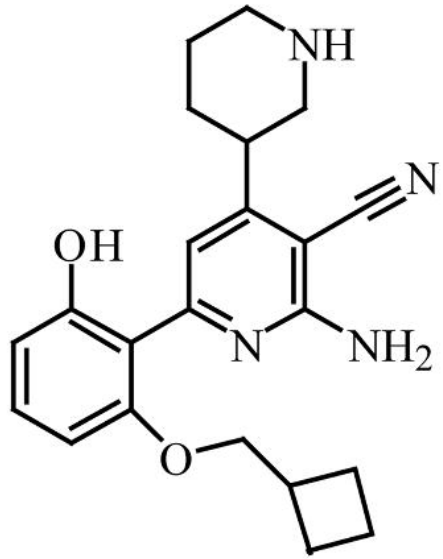
NH
N
OH
N
NH2
O

Fig 5

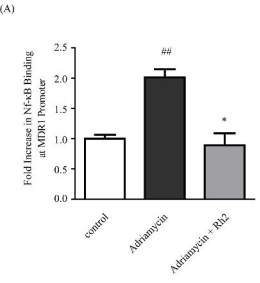
(A)
Fold Increase in Nf-κB Binding at MDR1 Promoter
2.5
2.0
1.5
1.0
0.5
0.0
##
*
control
Adriamycin
Adriamycin + Rb2

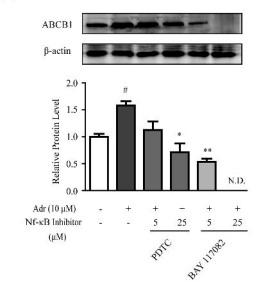
(B)
ABCB1
β-actin
Relative Protein Level
2.0
1.5
1.0
0.5
0.0
#
*
**
N.D.
Adr (10 μM) - + + - + +
Nf-κB Inhibitor (μM) - - 5 25 5 25
PDTC
BAY 117082

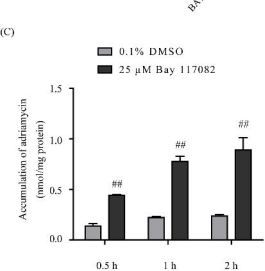
(C)
0.1% DMSO
25 μM Bay 117082
Accumulation of adriamycin (nmol/mg protein)
1.5
1.0
0.5
0.0
##
0.5 h
1 h
2 h

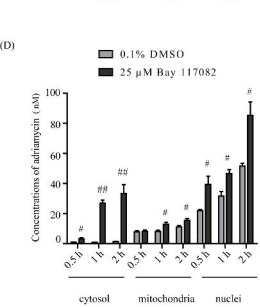
(D)
0.1% DMSO
25 μM Bay 117082
Concentrations of adriamycin (nM)
100
80
60
40
20
0
#
##
0.5 h
1 h
2 h
cytosol
mitochondria
nuclei

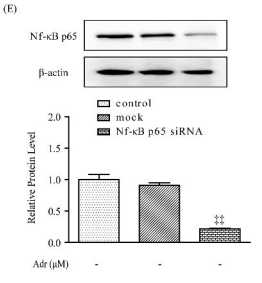
(E)
Nf-κB p65
β-actin
control
mock
Nf-κB p65 siRNA
Relative Protein Level
2.0
1.5
1.0
0.5
0.0
‡‡
Adr (μM) - - -

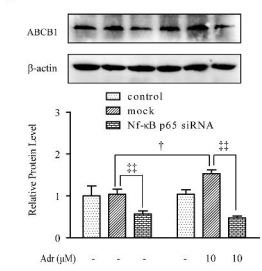
(F)
ABCB1
β-actin
control
mock
Nf-κB p65 siRNA
Relative Protein Level
3
2
1
0
†
‡‡
‡‡
‡‡
Adr (μM) - - - - 10 10

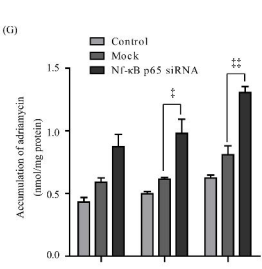
(G)
Control
Mock
Nf-κB p65 siRNA
Accumulation of adriamycin (nmol/mg protein)
1.5
1.0
0.5
0.0
‡
‡‡
0.5 h
1 h
2 h

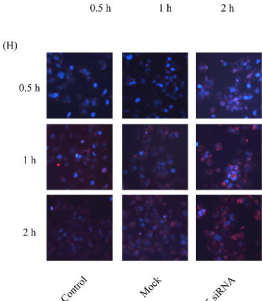
(H)
0.5 h
1 h
2 h
Control
Mock
Nf-κB p65 siRNA

Fig 6

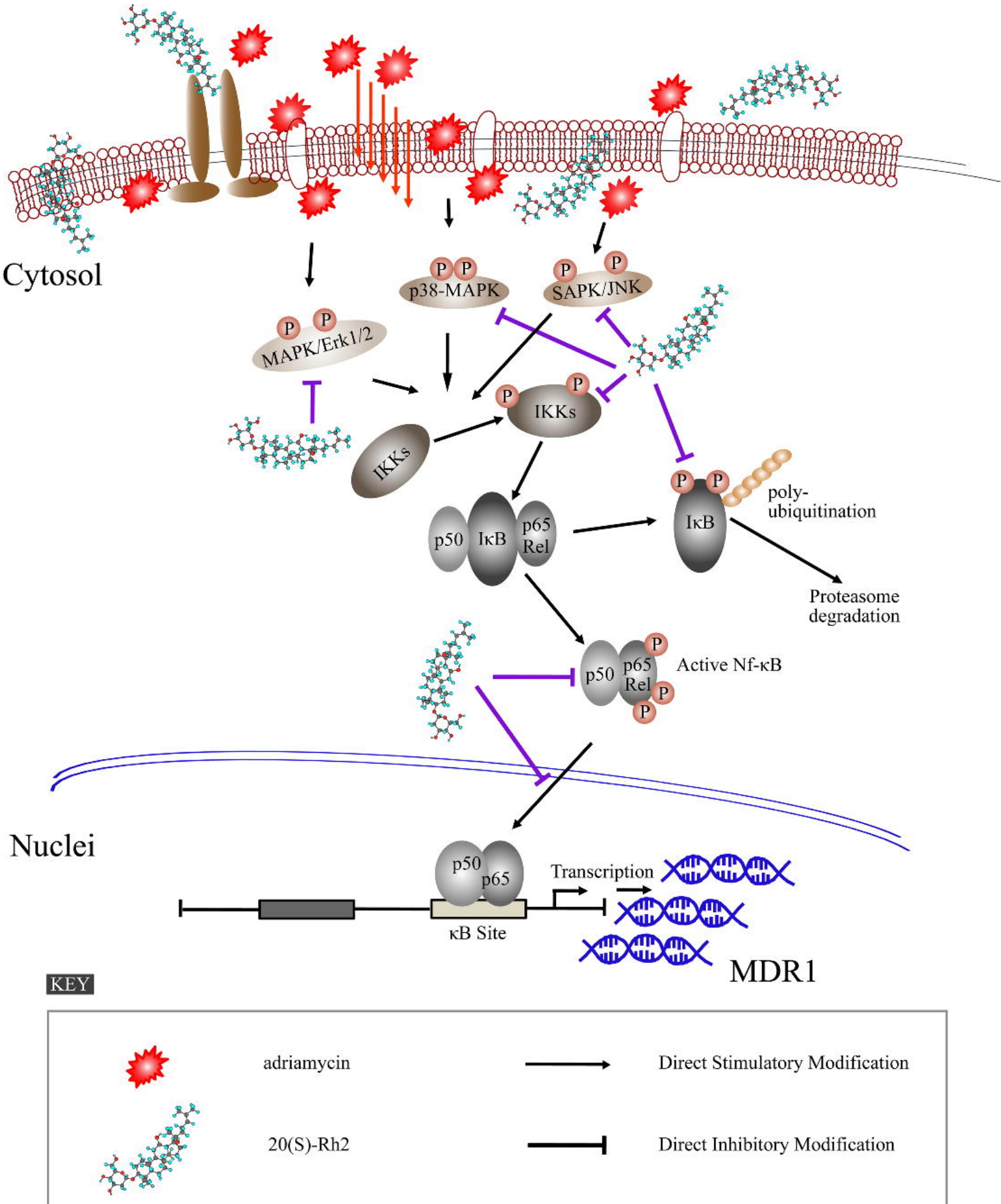
Cytosol
P P
p38-MAPK
P P
SAPK/JNK
P P
MAPK/Erk1/2
P P
IKKs
IKKs
p50 IκB p65 Rel
P P
IκB
poly-
ubiquitination
Proteasome
degradation
p50 p65 Rel
P
Active Nf-κB
Nuclei
p50 p65
Transcription
κB Site
MDR1
KEY
adriamycin
Direct Stimulatory Modification
20(S)-Rh2
Direct Inhibitory Modification